Kuhlmann, J., Dobslaw, H., Petrick, C., Thomas, M. (2013): Ocean bottom pressure signals around Southern Africa from in situ measurements, satellite data, and modeling. - *Journal of Geophysical Research*, *118*, 10, 4889-4898

DOI: 10.1002/jgrc.20372

JOURNAL OF GEOPHYSICAL RESEARCH: OCEANS, VOL. 118, 4889–4898, doi:10.1002/jgrc.20372, 2013

Ocean bottom pressure signals around Southern Africa from in situ measurements, satellite data, and modeling

Julian Kuhlmann,[1,2] Henryk Dobslaw,[1] Christof Petrick,[1,2] and Maik Thomas[1,2]

Received 13 March 2013; revised 22 August 2013; accepted 24 August 2013; published 2 October 2013.

[1] Ocean bottom pressure (OBP) variability in the region of the Agulhas Current off the South African coast is a crucial variable in the understanding of dynamic processes in the ocean, but measurements currently available lack either precision or spatial and temporal coverage. We provide a quantitative estimate of OBP variability throughout the region with the help of a setup of the ROMS regional ocean model. Driving the model with boundary conditions from a global ocean model and atmospheric reanalysis data and running it for 8 years, we are able to reproduce many characteristic properties of the regional ocean circulation visible in sea surface height and OBP fields. While the in situ pressure-inverted echo sounders (PIES) measuring local OBP variations on short time scales are sparse in the region, our model provides a comprehensive estimate of OBP variations throughout the region which reach values of up to 15 hPa when barotropic Agulhas rings reach the Cape Basin. These signals turn out to be difficult to measure with current gravimetry solutions from the GRACE satellites, but estimates of localized noise levels for a GRACE follow-on mission let the search for them in future satellite measurements appear viable.

Citation: Kuhlmann, J., H. Dobslaw, C. Petrick, and M. Thomas (2013), Ocean bottom pressure signals around Southern Africa from in situ measurements, satellite data, and modeling, *J. Geophys. Res. Oceans*, *118*, 4889–4898, doi:10.1002/jgrc.20372.

1. Introduction

[2] Global mean sea level rise during the past two decades has been fairly constant at about 3.2 mm/yr [*Meyssignac and Cazenave*, 2012]. Locally, however, the signal varies greatly. The various causes for sea level changes, e.g., heat input from the atmosphere, freshwater input from the cryosphere, river discharge, or changes in ocean currents, leave different regional footprints in the sea level distribution. One way of separating the different physical mechanisms that lead to sea level variability is to distinguish between steric, i.e., density-driven, and eustatic, i.e., mass-driven changes. The vertically integrated density field is measured as ocean bottom pressure (OBP), either by in situ pressure sensors [e.g., *Baker-Yeboah et al*., 2010] on the seafloor or by remote sensing devices such as the GRACE satellites [*Chambers et al*., 2004].

[3] Beyond the attribution of sea level rise to specific causes, a better understanding of this variable is also crucial for the understanding of ocean dynamics: variations of barotropic currents leave a signal in the OBP field. Furthermore, the processing of gravitational measurements, either in situ on land [e.g., *Kroner et al*., 2009] or with the GRACE satellites [e.g., *Dobslaw and Thomas*, 2007], depends on high-quality OBP products in order to separate contributions to the gravimetrical signal from different sources such as ice mass changes, hydrology, or crustal deformation. Up to now, those gravimetrical data sets have mostly relied on coarse ocean models in the assumption that mass variations on smaller scales are negligible. With improvements in accuracy of the measurements and reductions of errors from other sources, this assumption may, however, lose its justification.

[4] The high resolution required to resolve small-scale OBP signals makes regional ocean models a powerful tool for flexible investigations. The region we focus on is the surroundings of Southern Africa, dominated by the Agulhas Current and its retroflection. The Agulhas Current flows from the Mozambique Channel southward, along the African coast, toward the Cape of Good Hope. At around 34°S, it separates from the coast and continues to flow southwestward [*Lutjeharms et al*., 1989]. When it reaches about 40°S, most of the water masses change direction and are deflected toward the Indian Ocean. At this point, rotating mesoscale structures called Agulhas rings can be either shed into the South Atlantic or change their path and follow the Agulhas retroflection, which flows parallel to the Antarctic Circumpolar Current (ACC) back eastward toward the Indian Ocean. The amount of warm and saline water leakage into the Atlantic is still a topic of dispute [*van Sebille et al*., 2009; *Biastoch and Böning*, 2013], also due to its possible impacts on global climate [*Beal et al*., 2011]. Since the Agulhas region is rich in mesoscale eddies

[1]Geodesy and Remote Sensing, Section 1.3: Earth System Modelling, GFZ German Research Centre for Geosciences, Potsdam, Germany.
[2]Freie Universität Berlin, Institute of Meteorology, Berlin, Germany.

Corresponding author: J. Kuhlmann, GFZ German Research Centre for Geosciences, Section 1.3, Earth System Modelling, Telegrafenberg, A20 313, 14473 Potsdam, Germany. (julian.kuhlmann@gfz-potsdam.de)

2169-9275/13/10.1002/jgrc.20372

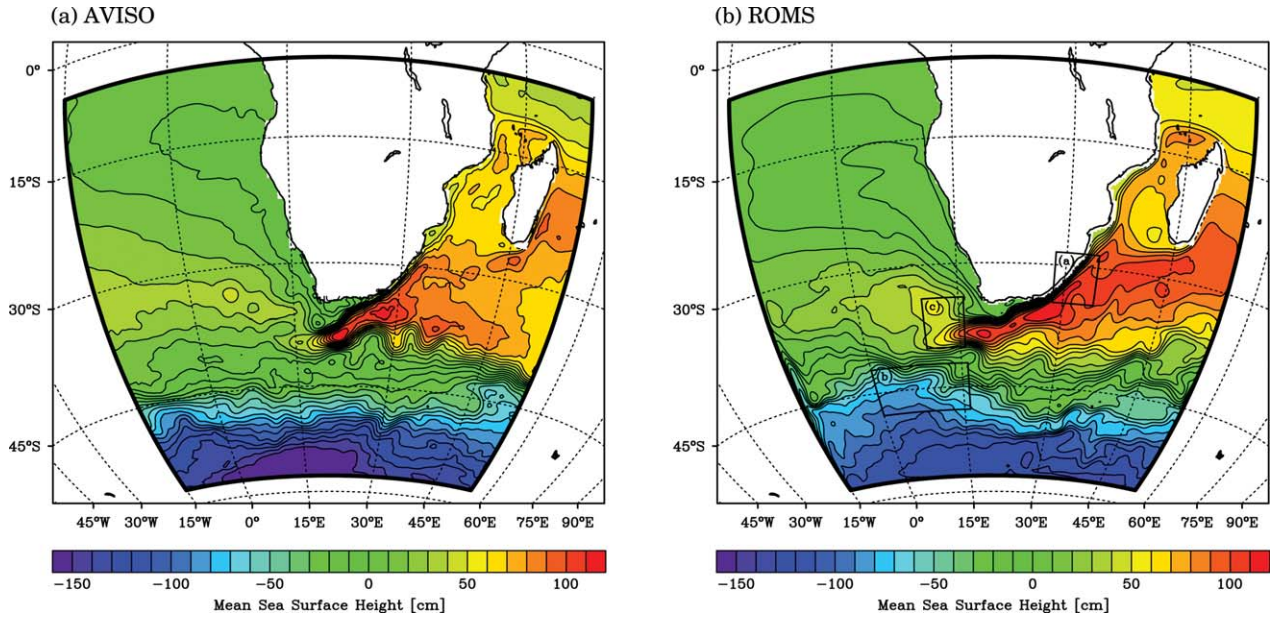

Figure 1. Mean detrended sea surface height during the time period of 2003–2008 (a) in the AVISO satellite altimetry data and (b) in our configuration of the ROMS model. Both data sets have been brought to a similar spatial average value in order to make them comparable. The black boxes in Figure 1b indicate the areas investigated further in Figure 3.

[*Doglioli et al*., 2007], it is a prime example for the use of regional numerical ocean models that can run at a higher resolution than their global counterparts. Modelling efforts by *Penven et al*. [2006] and *Rouault et al*. [2009] have focused on the immediate surroundings of the Southern African continent. *Byrne and McClean* [2008] have shown that in a comparison of a high-resolution global model to satellite altimetry data that much of the local variability is not adequately captured by the satellites. In situ measurement campaigns have attempted to quantify Agulhas Current transport [*Bryden et al*., 2005], regional tides [*Ray and Byrne*, 2010], and to track and investigate individual eddy structures [*van Aken et al*., 2003; *Froyland et al*., 2012]. Despite increasing research efforts, however, even basic characteristics of the Agulhas Current such as the existence of a seasonal cycle are up for debate [*Krug and Tournadre*, 2012].

[5] *Baker-Yeboah et al*. [2009] analyzed local OBP variations in detail using in situ data from 12 devices measuring a cross section of the eddy corridor through which shedding toward the South Atlantic occurs. They investigated the density structure of the eddies and determined that, in contrast to other eddy-intensive regions in the world such as the Kuroshio, the Agulhas rings often have a strong barotropic component, thus leaving a trace in OBP measurements. In order to determine this mass-induced signal, giving hints about the vertical structure of eddies, altimetric measurements need to be complemented by in situ or satellite-derived OBP signals.

[6] Our investigations focus on the modelling and observation of OBP in the Agulhas Current region. We will investigate local OBP measurements provided by in situ pressure-inverted echo sounders (PIES) as well as global OBP measurements with the GRACE satellites. These two data sets show stark disagreements due to the different spatial scales they capture. In order to resolve this conflict and to come up with an estimate of the magnitude and extent of OBP variations throughout the Agulhas region more precise than GRACE data, but at the same time, more comprehensive than sparse in situ measurements, we configure a setup of the regional ocean model ROMS [*Shchepetkin and McWilliams*, 2005] to simulate mesoscale ocean dynamics around South Africa. After having validated our model setup with satellite altimetry data, we will examine the strongly differing local OBP variabilities measured at the different PIES in the context of our simulation of the dynamics. We will then explore the current technical limitations of GRACE data to detect the Agulhas ring-induced OBP signals the PIES measure and discuss the prospects of satellite gravity data available in the future to capture them.

2. Model and Data

2.1. Ocean Model

[7] The Regional Ocean Modeling System (ROMS) [*Shchepetkin and McWilliams*, 2005] is a three-dimensional, free-surface, mode-splitting ocean model available free of charge under an open-source license (http://myroms.org/). It solves the primitive equations on terrain-following vertical coordinates and has been applied by the scientific community to a wide variety of scenarios ranging from local simulations spanning a few tens of kilometers [e.g., *Drews and Han*, 2010] up to global simulations [e.g., *Song and Colberg*, 2011].

[8] Our ROMS setup simulates ocean dynamics in a study area stretching from 57.5°S to 5°S and from 15°W to 55°E (Figure 1). Thereby we include, besides the Agulhas

Current itself, its confluence from the Mozambique Channel where the Natal pulses originate, the outflow toward the South Atlantic, and a segment of the ACC where in situ OBP measurements have been taken with PIES [*Macrander et al*., 2010]. The horizontal resolution of the model setup is 0.20° in latitudinal and 0.25° in longitudinal direction. Vertically, we split the water column into 32 layers, their thickness increasing with depth.

[9] Internally, one baroclinic model time step lasts 10 min; the barotropic time steps are 15 times shorter. The modeled temperature, salinity, horizontal and vertical velocities, and sea surface height (SSH) fields are averaged over one day and then stored for later analysis. The spatial distribution of ocean bottom pressure is computed in the postprocessing from the 3-D density distribution, the sea level fields, and local depth. We are interested in local rather than domainwide mass variations, since the latter can be more appropriately modeled with a global ocean model, so we remove variations of the total ocean mass from the data.

[10] Horizontal eddy viscosity is parameterized following *Smagorinsky* [1963]. We chose a value of 0.0125 as the Smagorinsky parameter, thereby producing mesoscale eddies of sizes and magnitudes close to what has been observed by satellite altimetry. A fourth-order Akima scheme deals with horizontal and vertical tracer advection in addition to a generic length scale mixing parameterization [*Umlauf and Burchard*, 2003].

[11] The boundary conditions at the domain's four open boundaries come from global simulations with the ocean model for circulation and tides (OMCT) [*Thomas et al*., 2001] run at $1.875° \times 1.875°$, linearly interpolated onto the terrain-following ROMS coordinates with a MATLAB toolbox designed by *Penven et al*. [2008] for that purpose (http://www.romsagrif.org). We apply daily mean values of horizontal velocities, temperature, and salinity as well as barotropic momentum and sea surface height. As atmospheric forcing we use 6-hourly wind stresses and net freshwater fluxes from the atmosphere as well as 3-hourly surface heat flux from the ERA-Interim reanalysis [*Dee et al*., 2011]. The same data set has been used to drive the OMCT simulations for the boundary conditions. Information about the local bathymetry comes from the ETOPO2 data set (http://www.ngdc.noaa.gov/mgg/global/etopo2.html). Note that the OMCT simulation providing the boundary conditions does not include tides, since the focus of our study is the general circulation only.

[12] The initial fields of temperature and salinity for the model run come, in accordance with the boundary conditions, from OMCT results interpolated on the ROMS grid. Velocities and SSHs start from zero since the different spatial scales of resolved phenomena would make OMCT results rather inadequate for the ROMS grid. We begin the model run on 1 January 2001 and let the model run for 2 years, forced by atmospheric and oceanic boundary data, as a spin-up. These first 2 years are not analyzed further. Even though large-scale circulation adapts to the T and S initialization fields within days, these 2 years are needed to produce mesoscale circulation, since meander modes originating from the Mozambique Channel and Agulhas rings spawned from the retroflection south of Cape Town need several months to travel through the region. We then extend the model run by 6 years which we analyze. Our study period therefore comprises the years 2003–2008.

2.2. Observational Data

[13] In order to ground our analysis in measurements of the magnitudes in question, we make benefit from the work done by the Archiving Validation and Interpretation of Satellite Data in Oceanography (AVISO) project (http://www.aviso.oceanobs.com/duacs). In the AVISO data, satellite altimetry observations from various instruments and platforms are gathered into a single data set, providing a continuous record of daily global sea level fields at 1/3° horizontal resolution. Although the data we use is provided on daily fields, the repeat cycles of the satellite tracks prohibit the extraction of meaningful signals on time scales smaller than a week. AVISO data exist from 1992 up to today.

[14] Satellite data of OBP comes from the Gravity Recovery and Climate Experiment (GRACE). The satellite pair uses intersatellite distance to estimate the gravitational effect of mass redistribution within the Earth system. We use the ITG-Kalman solutions provided by the Institut für Theoretische Geodäsie, University of Bonn [*Kurtenbach et al*., 2009]. The ITG-Kalman data are based on a Kalman Smoother approach in order to come up with daily fields of mass variations in form of spherical harmonics up to degree and order 40, corresponding to a horizontal resolution of approximately 500 km. Model-based estimates for continental, atmospheric, and solid Earth contributions have been subtracted from the initial data, so we retain a purely oceanographic signal. The ITG-Kalman data are available from August 2002 on.

[15] OBP is further measured by PIES, in situ devices placed on the seafloor by Alfred-Wegener Institute [*Macrander et al*., 2010], Proudman Oceanographic Laboratory [*Rietbroek et al*., 2006], and Centre National d'Etudes Spatiales (see http://www.psmsl.org/links/programmes/acclaim.info.php). These PIES, located at 12 positions in or around our model domain, record OBP variations at a temporal resolution of 30 min. We have detrended the data in order to account for the sensor drift common to these instruments, removed the tidal signals with a Doodson X0 filter and then computed daily averages of the signal. The length of the time series varies from device to device, reaching from 1 to 3 years. The PIES measurements are therefore most suited for the investigation of signals on annual or shorter time scales. Locations and time periods for which data is available can be found in Table 1.

3. Results

3.1. Initial Model Evaluation

[16] We evaluate the model setup by comparing its output with a well-established satellite altimetry data set. Satellite altimetry, measuring the elevation of the sea surface, has been available for two decades and has been widely applied to describe ocean dynamics, also in the region of this study [*Krug and Tournadre*, 2012; *Byrne and McClean*, 2008]. We therefore expect that, once the model reliably reproduces patterns of sea level distributions and their variability as integral measures of ocean dynamics, it is also trustworthy in simulating variables linked to ocean

Table 1. In Situ OBP Measurements Collected by AWI Bremerhaven[a]

PIES ID	Latitude	Longitude	Start Date	End Date	n
AWI ANT3	37.09°S	12.77°E	7 March 2007	8 February 2008	339
AWI ANT5	41.13°S	9.94°E	29 January 2005	9 February 2008	1107
AWI ANT537	41.18°S	4.26°E	30 August 2006	8 February 2008	528
AWI ANT7-1	44.66°S	7.08°E	29 November 2002	26 January 2005	790
AWI ANT7-2	44.66°S	7.08°E	29 January 2005	11 February 2008	1109
AWI ANT9	47.66°S	4.26°E	1 February 2005	13 February 2008	1108
AWI ANT10	49.01°S	2.83°E	14 December 2006	29 December 2007	381
AWI ANT11	50.26°S	1.43°E	1 December 2002	30 January 2005	792
AWI ANT13a	52.51°S	1.40°W	26 October 2006	17 February 2008	480
CNES CRO	46.55°S	51.79°E	24 January 2002	9 December 2004	1051
POL IO1	47.12°S	54.90°E	25 January 2004	15 February 2005	388
POL IO2	48.83°S	61.28°E	26 January 2004	29 January 2005	370

[a]In the last column, *n* is the number of days with OBP measurements that were evaluated. Except for *CNES CRO*, each PIES delivered data for more than 98% of the deployment time.

dynamics that evade direct measurement. Since a direct comparison of time series is not expected to yield meaningful results in the case of a nonassimilative model setup, we limit our comparisons to statistical quantities.

[17] The mean SSH measured by AVISO (Figure 1a) is reproduced by the mean SSH simulated by our ROMS setup (Figure 1b) in the crucial, large-scale features of the regional ocean dynamics: The SSH gradients show an Agulhas current of realistic strength, position, and extent; an ACC spanning the width of the region and following a path similar to what is observed, although somewhat less zonal; a retroflection transporting most of the Agulhas waters back toward the Indian Ocean; and a region of ring shedding in the South Atlantic. The features are generally more washed out than they are even in a 6 year mean of the observations, which nevertheless has to be expected when using a model of 0.25° resolution. There is a discontinuity between the ACC inflow at the western boundary between 35°S and 55°S in the OMCT boundary conditions and the interior ACC simulation. Since the atmospheric forcing is the same, this must be a result of interior dynamics, presumably due to the different spatial scales resolved. It could also be that different implementations of vertical momentum transport lead to a less vigorous ACC in the global OMCT model. Fortunately, the modeled ACC picks up speed quickly after having entered the model domain, so the boundary artifacts influence only a small area. Outside of this specific section of the western boundary, the transitions from boundary data to interior data are fairly smooth.

[18] Since we aim at reproducing the variations of ocean currents in time, the modeled SSH standard deviation field needs to be close to what has been measured as well. While the model output comes in daily average fields, the effective temporal resolution of the AVISO satellite data is

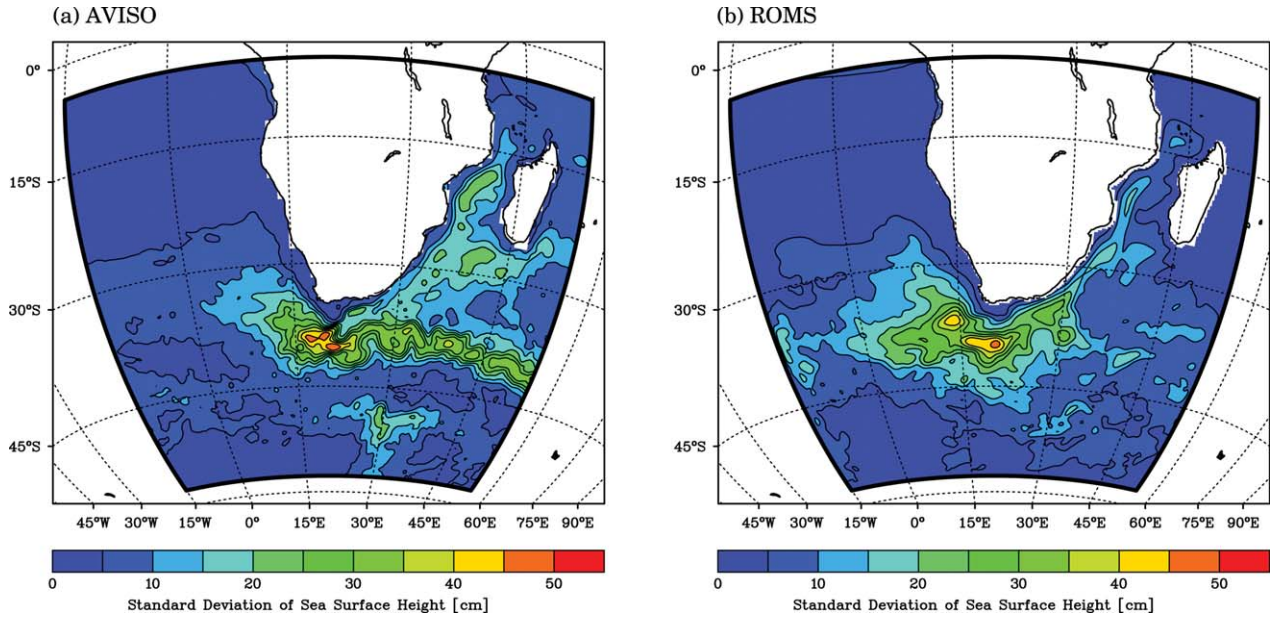

Figure 2. Standard deviation of detrended sea surface height weekly means during the time period of 2003–2008 (a) in the AVISO satellite altimetry data and (b) in our configuration of the ROMS model.

weekly, so we first filter the model output in time to make both data sets comparable. Examining the two fields in Figures 2a and 2b, we can identify a region of maximum variability in the eastern Cape Basin, where SSH standard deviation reaches values of up to 50 cm. This is the area of strong eddy activity mostly originating from Agulhas ring shedding which has been dubbed "Cape Cauldron" due to the vigorous mixing [*Boebel et al*., 2003]. The surrounding area of increased turbulence comprises parts of the South Atlantic that are slightly more vast in the simulation than in the observations. Also, in the model, the increased variability reaches more westward, while the observations show more of a northwestward extension of this zone, hinting at a difference in the path of outgoing Agulhas rings. The variability within the Agulhas Current, from the Mozambique Channel southward to the Cape region, is very similar in model and observation. A stark difference is apparent along the 40°S latitude band, where retroflected eddies and current meandering lead to a standard deviation in the observations of around 30 cm, while the Return Current in the model is less turbulent with a standard deviation of only 10 cm. Since our focus in this study lies on the central and western part of the study region, this deficiency can however be tolerated. Furthermore, the comparison of mean SSH fields showed that at least the mean slope of the Agulhas Return Current in the model is reasonable, so reduced variability here should not be detrimental to investigations upstream.

[19] Similar standard deviations can, however, result from variability in very different frequency bands. To investigate whether this is the case, in Figure 3 we show spectra of SSH variability in three representative areas indicated in Figure 1b: (a) within the Agulhas Current ($31.5 \pm 3°$S, $31.5 \pm 3°$E), (b) along a part of the ACC ($45 \pm 3°$S, $8 \pm 12°$E), and (c) around one of the in situ measurements that will be analyzed later ($37 \pm 3°$S, $12.75 \pm 3°$E). In both the Agulhas Current and the ACC, the model reproduces the dominant seasonal signal apparent in the satellite data. In the Agulhas Current (Figure 3a), also a semiannual signal with an amplitude of 20 cm and peaks at shorter periods are correctly captured by the model. On interannual periods, however, the model shows more variability than the satellite data. Meanwhile, on periods of a month and less, the variability the model produces cannot be captured by the satellites due to their slow repeat cycle. This observation is similar to the conclusions of *Byrne and McClean* [2008] for the Agulhas region and is also apparent in the data from the ACC section (Figure 3b), where the model shows signals on periods below 30 days that are not measured by the satellites. Interannual variability is captured well here with both spectra flattening out at 30 cm. Off the Cape of Good Hope (Figure 3c), the model slightly overestimates the variability on submonthly time scales while underestimating it on periods of a year and more. On periods between a month and a year, spectra of model and observation mostly do not differ significantly, even though specific features such as the weak annual peak in the observations cannot be reproduced unambiguously. The narrow confidence interval for the ROMS spectrum in Figure 3c originates from the shorter temporal autocorrelation length due to the model producing Agulhas rings rather regularly at periods between 1 and 4 months (0.08 and 0.33

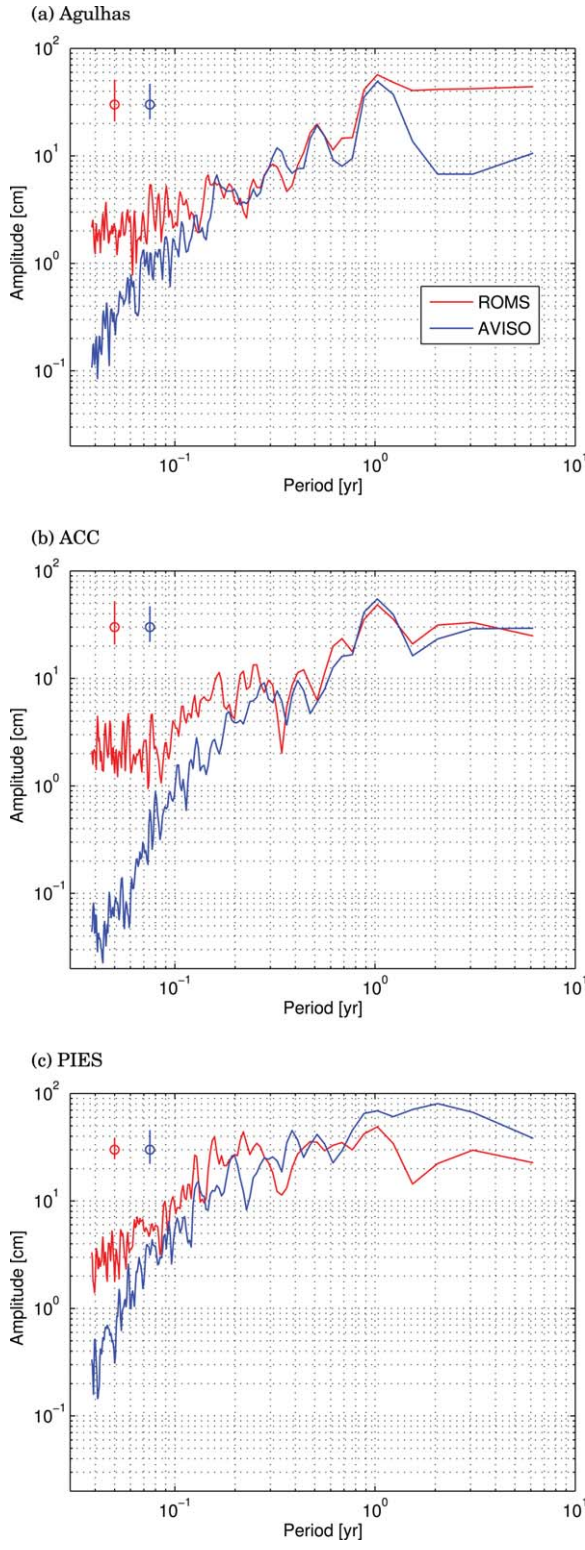

Figure 3. Spectra of sea surface heights in the ROMS model and in AVISO satellite data at the three different locations indicated in Figure 1b: (a) in the Agulhas Current ($31.5 \pm 3°$S, $31.5 \pm 3°$E), (b) in the ACC ($45 \pm 3°$S, $8 \pm 12°$E), (c) around one of the in situ OBP measurement sites ($37 \pm 3°$S, $12.75 \pm 3°$E). In the upper left, the 99% confidence levels for each spectrum are indicated.

years), which is visible as elevated spectral density. Meanwhile, ring shedding in the observations is more chaotic and occurs on a wider range of periods. Overall, the spectral comparison of observational and model data shows good agreement, providing hints that the most important underlying physical processes are simulated properly in the model.

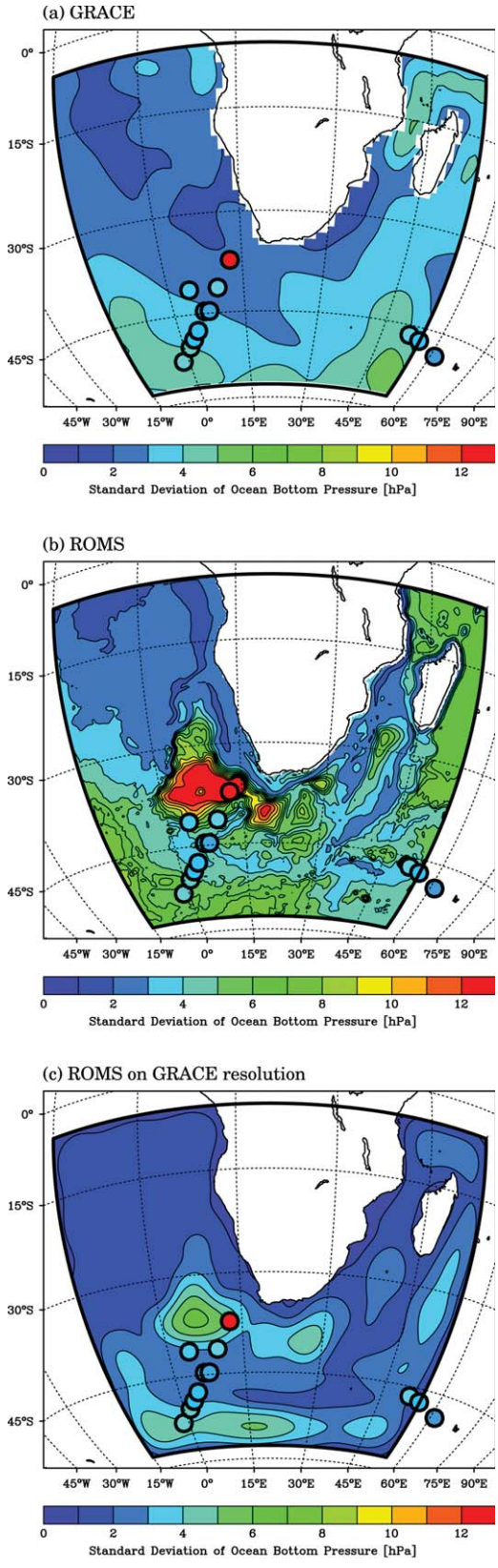

Figure 4. Standard deviation of daily ocean bottom pressure fields during the time period of 2003–2008 (a) in the ITG-Kalman solution, (b) in our configuration of the ROMS model, (c) in our configuration of the ROMS model with a cutoff at spherical harmonics degree and order 40 and as 10 day means. The filled dots show the standard deviations measured by in situ PIES.

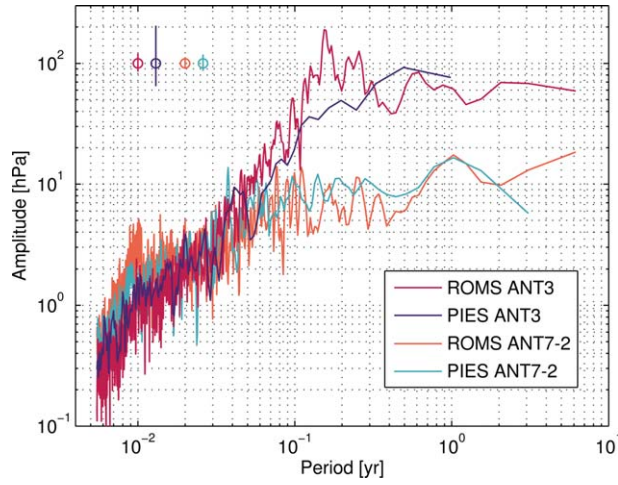

Figure 5. Spectra of OBP time series measured by the PIES ANT3 and ANT7-2 (see Table 1) compared to the ROMS simulations of OBP at the same locations. In the upper left, the 99% confidence levels for each spectrum is indicated.

3.2. OBP Signals in Observations and Model

[20] Figure 4a shows the standard deviations of daily OBP fields measured by the GRACE satellites (filled contours) and by in situ PIES (filled circles). These two measurement systems, although tracking the same variable, represent opposing extremes in spatial scales: The GRACE data has a nominal spatial resolution of roughly 500 km. Standard GRACE products provide a temporal resolution of 10 days to a month, and great efforts, including the application of a Kalman Smoother, had to be made to come up with global daily fields in the ITG-Kalman solution [*Kurtenbach et al*., 2009]. The decorrelation scales in space and time for the process model of the Kalman Smoother have been taken from the OMCT ocean model. Meanwhile, the PIES are indicative of OBP variations at a very specific location each and deliver data every 30 min; the standard deviations in Figure 4a originate from data from which the tides were removed with a Doodson X0 filter [*Doodson and Warburg*, 1941] before daily averages were computed. That said, the comparison shows certain common features. In the GRACE data, apart from stronger variability in the Indian Ocean, a north-south gradient going from an OBP standard deviation of below 3 hPa in the Tropical Atlantic to around 5 hPa south of 45°S is the dominant feature. This gradient is somewhat found again in the PIES data southwest of South Africa, at least in the signals from the

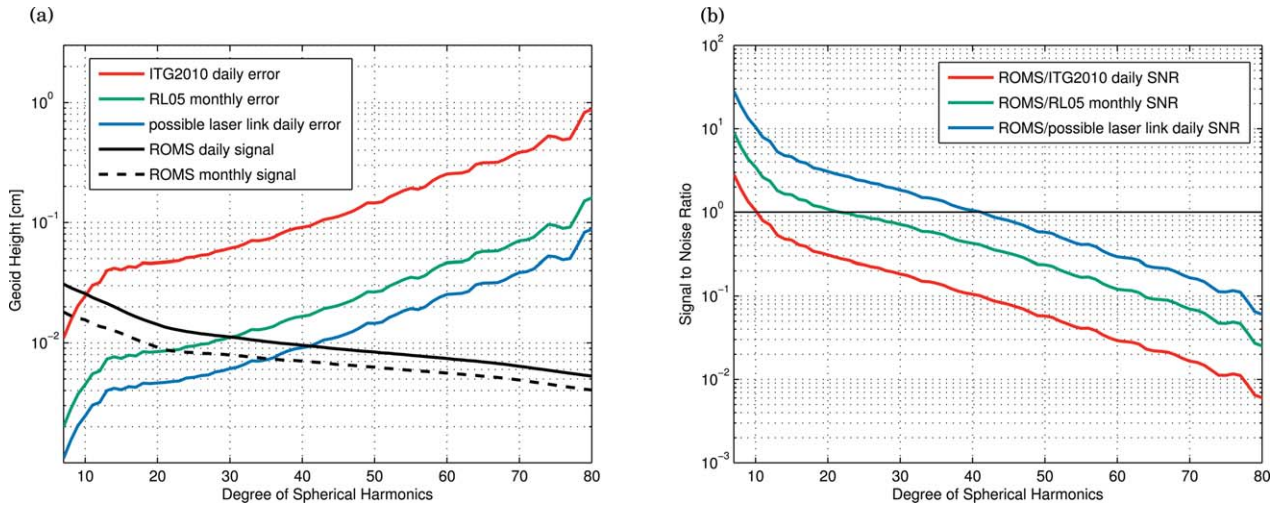

Figure 6. Estimates for (a) the degree-dependent noise level of GRACE measurements limited to the study domain as well as the amplitude of the signal derived from the ROMS model runs and (b) the resulting signal-to-noise ratios, with the black line indicating an SNR≡1.

devices "AWI ANT7-1" through "AWI ANT13a." There is but one notable exception from this pattern: The in situ device "AWI ANT3" at 37.09°S, 12.77°E, measuring an OBP variability of 12.5 hPa. This stands out in comparison to both the GRACE data and the other PIES, which all remain around 3–4 hPa. It is in agreement, however, with the data presented by *Baker-Yeboah et al*. [2009] for an earlier time period.

[21] Replacing the GRACE OBP with the modeled OBP standard deviations (Figure 4b), it is apparent that certain broad-scale features are well reproduced: The north-south gradient in the Atlantic, as well as increased variability in the Indian Ocean, that GRACE observes are visible in the model simulations. In both cases, the agreements need to be interpreted with caution, since boundary effects might also play a role in their formation. In the case of the Indian Ocean, unfortunately, the lack of PIES leaves us in the dark about whether boundary effects in the simulations, leakage effects in the GRACE data, or physically meaningful ocean variations dominate the variability there. This cannot be said about the strong OBP variability throughout the Cape Basin in the model simulations (between 0° and 15°E, 25°S and 40°S). Here, the ROMS setup produces OBP variability up to 15 hPa, compared to roughly 2.5 hPa in the GRACE data. This area is precisely where the PIES "AWI ANT3" mentioned above is situated, leading us to place confidence in the simulated strong variabilities. The barotropic nature of many Agulhas rings in the Cape Basin has been repeatedly reported in the literature. For example, *van Aken et al*. [2003] investigated a particular Agulhas ring during a cruise in the year 2000 and showed it to produce currents down to the seafloor. While focussing on a later stage of the lifetime of Agulhas rings, *van Sebille et al*. [2012] investigated the dynamics involved in great detail.

[22] The ITG-Kalman solution has a horizontal resolution of roughly 500 km, and while it delivers daily average fields, the repeat cycle of the GRACE satellites is much slower, leading to standard GRACE products being delivered only as 10 day mean fields. In order to make the model output more comparable to the GRACE data, we developed it in spherical harmonic functions, set all coefficients beyond degree and order 40 equal to zero, resynthesized them into the spatial domain, and computed 10 day mean fields. The standard deviation of this mockup satellite data is shown in Figure 4c. Compared to Figure 4b, the east-west and north-south gradients are dampened but still visible, even though the spatial smoothing of the fields produces artificially low variability at the edges of the study domain. The amplitudes of around 5 hPa in the Southern and Indian Oceans are close to what is observed by GRACE in Figure 4a. The high OBP variability in the Cape Basin, however, withstands the smoothing. Its amplitude decreases to around 7 hPa (compared to 15 hPa before the smoothing) but is still the dominant signal in the model output. It is therefore probably not purely due to limited temporal and spatial resolution of the GRACE data that the Agulhas rings are not detected.

[23] In order to judge whether the model simulations of OBP variability agree with the PIES measurements not only in standard deviation, but also in spectral content at different periods, we show the spectra of the signals in Figure 5 for two of the measurement locations, ANT3 and ANT7-2 (see Table 1). Beside the general redness of the spectra, it is also apparent that the model succeeds in simulating the similar variability at periods from days to about a month and the almost tenfold predominance of the amplitude at periods longer than 1 month at the site ANT3 compared to ANT7-2. The annual signal at the location of ANT7-2 is accurately simulated by ROMS. Such a signal is absent from the simulation at ANT3 and cannot be detected from the short PIES time series here, which also leads to the broad confidence interval for this spectrum. At periods between 1 and 4 months (0.08 and 0.33 years), the modeled spectrum deviates from the measurements. The peaks here are related to the formation of barotropic Agulhas rings in the model. Too regular ring formation is a shortcoming that many numerical ocean models of the region share [*Lutjeharms and Webb*, 1995; *Backeberg et al*., 2009].

Nevertheless, the frequency of ring formation is, with about five rings shed per year, in accordance with estimates from the literature [*van Aken et al*., 2003]. The decent overall correspondence in a statistical sense throughout much of the spectrum and also at short periods leads us to believe that the model simulates the local processes governing OBP variability reasonably well and is therefore capable to provide useful quantitative estimates of OBP variability also at locations where no in situ measurements are available.

3.3. Detectability of Agulhas Ring-Induced OBP Signals With GRACE

[24] Consistently with the published literature [*Byrne and McClean*, 2008; *Baker-Yeboah et al*., 2009], our model simulations show an OBP signal above 10 hPa of standard deviation caused by Agulhas rings in the Cape Basin. The signal is simulated to spread throughout the basin in a way that, considering temporal and spatial resolution, it should be detected by GRACE. The ITG-Kalman data, however, shows otherwise.

[25] There are various possible causes for the discrepancy between model and in situ data on the one hand and satellite data on the other hand. First, the GRACE satellites measure a gravitational signal of both the continental hydrology and ocean mass variations, with the hydrological signal being about three times as strong as the oceanic signal. While the ITG-Kalman solution we use is a pure ocean product, thus attempts have been made to remove the hydrological signal from the data, the proximity of the Cape Basin to the South African coast (about 600 km) could lead to a loss of signal due to exaggerated removal of meaningful ocean mass signal in the GRACE postprocessing. Furthermore, the distribution of the GRACE satellite tracks can lead to redundant data at some points and an undersampling of the signal at others. Another culprit may be the background ocean model OMCT, whose covariance matrix was used for the Kalman Smoother approach producing the ITG-Kalman solutions. Since Agulhas rings are not present in the OMCT simulations, it is likely that ITG-Kalman underestimates them too.

[26] Many errors of the GRACE data, however, are well known and quantified. Noise levels for GRACE products are commonly given as a function of spatial scale in terms of the degree of spherical harmonic functions. These noise levels can be compared to the expected signal from a certain geophysical process. A signal-to-noise ratio (SNR) of more than 1 is needed to detect a signal in principle, although generally an SNR higher than that will be necessary to measure a signal reliably.

[27] In the case of the highly localized bottom pressure signals we are interested in, additional effort has to be put into the estimation of the SNR. *Wieczorek and Simons* [2005] and *Han and Ditmar* [2007] showed how the spherical harmonics spectrum of a signal can be localized by applying a window function to both the signal and the error fields. The window function is chosen in a way that the signal is present in the window only, while the error, by its nature, spans the entire globe. Therefore, the localization can increase the SNR above the threshold of detectability. We follow the same approach and show localized signal and error functions in Figure 6a as well as the resulting SNRs in Figure 6b. Since GRACE data is commonly distributed in terms of spherical harmonics describing the time-variable gravitational potential that can be displayed as changes in geoid height, the OBP fields need to be transformed into this quantity, too. This is done by first developing the field of surface mass density in spherical harmonic functions and then applying the relation

$$\begin{Bmatrix} C_{lm} \\ S_{lm} \end{Bmatrix} = \frac{3\rho_w}{\rho_{\text{ave}}} \frac{1+k_l}{2l+1} \begin{Bmatrix} \hat{C}_{lm} \\ \hat{S}_{lm} \end{Bmatrix} \tag{1}$$

from *Wahr et al*. [1998] to transform the coefficients of surface mass density $\hat{C}_{lm}$ and $\hat{S}_{lm}$ of degree l and order m into the geoid coefficients C_{lm} and S_{lm} using the density of sea water ρ_w, the average density of the Earth ρ_{ave}, and the degree-dependent load Love numbers k_l [see *Farrell*, 1972]. This transformation leads to the degree variances of the signal decreasing with increasing spherical harmonics degree l. GRACE noise levels, on the other hand, increase with increasing degree except for the first couple of degrees that lose much of their weight in the process of localization. Therefore, only the low-degree parts of the signal are expected to be measurable by GRACE.

[28] In Figure 6a, we show localized degree variances derived from our model output both for daily fields and monthly averages thereof. The temporal averaging reduces the signal by about a third. We base our comparison on a noise curve that belongs to monthly means of GRACE release 5 (RL05) data [*Dahle et al*., 2013]. In order to obtain a noise estimate for the daily ITG2010 data, we multiply it with a factor of $\sqrt{30}$ (T. Mayer-Gürr, personal communication, 2013), thereby accounting for the smaller amount of observational data incorporated into one daily field. The standard error of the mean decreases with the square root of the sample size, and for daily fields, only 1/30-th of the data is available compared to monthly fields. Multiplying this curve with a factor of 0.1 gives us the expected noise level for a possible follow-on GRACE mission. A tenfold error reduction is a rough estimate expected due to the implementation of more precise satellite ranging conducted with a laser instead of with microwaves as in the current system.

[29] Considering the SNR curve for the current ITG-Kalman product in Figure 6b, we see that the simulated gravity signals are currently detectable, if at all, only when they exceed a spatial scale of 2000 km (corresponding to degree 10), which Agulhas rings certainly do not. The detectability of simulated oceanic signals gets better for the monthly GRACE data, allowing for signals down to a scale of 1000 km (degree 20). This comes closer to the actual diameter of Agulhas rings, which can be hard to determine precisely *Schouten et al*. [2000], but has been estimated to around 300 km [*Lutjeharms*, 1981; *Schouten et al*., 2003]. Unfortunately, the monthly averaging of the GRACE data conflicts with the transient nature of the phenomenon. Nevertheless, improved reprocessing of the current GRACE measurements may bring the errors down just enough to measure at least large, strongly barotropic rings. The hope for GRACE measurements of Agulhas rings in the Cape Basin lie, however, in the GRACE follow-on mission with laser linkage. With a sensible compromise

between temporal and spatial resolution, OBP signals caused by Agulhas rings will be an ideal benchmark for this future satellite mission.

4. Summary

[30] We created a setup of the ROMS ocean model to simulate regional ocean dynamics around South Africa, including the Agulhas Current and a segment of the ACC. Results from an 8 year simulation have been validated with satellite altimetry, showing that the model setup is able to capture the essential features of ocean circulation in the region. The mean SSH field is well represented in the model. The standard deviations of SSH show maxima in the correct locations, with limits in the Return Current and the exact path of the ACC which are not further analyzed in this study. Spectral analysis of SSH variations in three representative locations show that variability in the model setup is occurring on the right time scales.

[31] Comparing fields of OBP variability from the model with gravimetric measurements from the ITG-Kalman solution and with in situ PIES bottom pressure signals, we corroborated the OBP simulated by the model at the locations where in situ measurements are available and identified a shortcoming of GRACE in measuring the strong OBP footprint of Agulhas rings in the Cape Basin.

[32] We finally explored the potential of current and future satellite gravimetry products to detect the simulated spatial distribution of OBP variability and show that the estimated accuracy of the planned GRACE follow-on mission will be just sufficient to measure the OBP footprint of large, barotropic Agulhas rings.

5. Conclusions

[33] This study adds to the existing work about ocean circulation throughout and around the Agulhas Current, one of the strongest currents in the world's oceans. It deals with ocean bottom pressure measured locally at a few locations throughout the region and globally with satellites. Combining these two independent measurements of the variable and extending the analysis with the aid of a regional ocean model, we provide an estimate of the location and amplitude of strong eddy-induced OBP signals throughout the region. The results can motivate future modeling efforts in the region focusing on geodetic observables, since they hint at an area of prominent mass variations on small scales.

[34] Simulations of ocean bottom pressure are also needed for the processing of satellite- and land-based gravity measurements that need to be corrected for ocean effects. While our model in the current nonassimilating setup cannot be used for dealiasing purposes, we showed that dealiasing products need to be obtained from high resolution, most likely regional, model setups in order to capture the strongest nontidal mass variations. Future solutions for the GRACE satellite data should be investigated for the presence of significant OBP signals off the South African coast, since new data processing algorithms might be able to measure signals here that, up to now, are most likely drowned in noise and smoothing. The signals identified take place on temporal (weeks to months) and spatial (hundreds of kilometers) scales that make them a promising objective for a GRACE follow-on mission.

[35] One immediate way to extend this study is to analyze longer measurement time series. An extension of the in situ OBP measurement time series would provide better estimates of the local spectra and make the identification of Agulhas rings in the OBP signal more reliable. More data from additional measurement sites might also hint at other interesting regions of nontidal OBP variability. For instance, the collection of data shown by *Macrander et al*. [2010] indicates that locations in or around the Kuroshio Current, the Malvinas Current, or the Drake Passage might be suitable as kinetic energy is high here as well [*Thompson and Demirov*, 2006].

[36] This study showed how Agulhas rings can leave a footprint in fields of OBP variability throughout the Cape Basin. Of course, other physical effects play a role for this variable, too. For instance, coastal and topographic features are accompanied by characteristic resonances that can be excited by local wind fields, an effect that would be superimposed on the turbulence-induced OBP variability. While the length scales and frequencies of the dominant OBP anomalies in our simulations show that the signals are predominantly eddy induced, a way to extend this study would be to separate and quantify these additional effects.

[37] Studies of OBP phenomena of the spatial extent of mesoscale eddies would also benefit from improved GRACE solutions. Especially, the planned GRACE follow-on mission, equipped with more precise laser satellite-satellite ranging instead of the current microwave-based system, might make it possible to bring all three data sets, GRACE, PIES, and ROMS, in agreement about OBP amplitudes off the South African coast.

[38] **Acknowledgments.** We wish to thank the ROMS developers (http://myroms.org/) around Hernan G. Arango at Rutgers University for providing the model code; Pierrick Penven at Centre IRD de Bretagne for sharing his ROMS Matlab Toolbox [*Penven et al*., 2008]; the team around Jens Schröter at AWI Bremerhaven, Germany, for providing the PIES data; Torsten Mayer-Gürr and his colleagues at the Institute of Geodesy and Geoinformation, University of Bonn, for their ITG-Kalman solutions; and Inga Bergmann-Wolf for her help in acquiring and preprocessing GRACE and PIES data. Furthermore, we are grateful for the comments from three anonymous reviewers, which helped to improve the manuscript considerably.

References

Backeberg, B. C., L. Bertino, and J. A. Johannessen (2009), Evaluating two numerical advection schemes in HYCOM for eddy-resolving modelling of the Agulhas Current, *Ocean Sci.*, *5*(2), 173–190, doi:10.5194/os-5-173-2009.

Baker-Yeboah, S., D. R. Watts, and D. A. Byrne (2009), Measurements of sea surface height variability in the eastern South Atlantic from pressure sensor-equipped inverted echo sounders: Baroclinic and barotropic components, *J. Atmos. Oceanic Technol.*, *26*(12), 2593–2609, doi:10.1175/2009JTECHO659.1.

Baker-Yeboah, S., D. A. Byrne, and D. R. Watts (2010), Observations of mesoscale eddies in the South Atlantic Cape Basin: Baroclinic and deep barotropic eddy variability, *J. Geophys. Res.*, *115*(C12), C12069, doi:10.1029/2010JC006236.

Beal, L. M., W. P. M. De Ruijter, A. Biastoch, and R. Zahn (2011), On the role of the Agulhas system in ocean circulation and climate, *Nature*, *472*(7344), 429–36, doi:10.1038/nature09983.

Biastoch, A., and C. W. Böning (2013), Anthropogenic impact on Agulhas leakage, *Geophys. Res. Lett.*, *40*, 1138–1143, doi:10.1002/grl.50243.

Boebel, O., J. R. E. Lutjeharms, C. Schmid, W. Zenk, T. Rossby, and C. Barron (2003), The Cape Cauldron: A regime of turbulent inter-ocean

exchange, *Deep Sea Res. Part II*, *50*, 57–86, doi:10.1016/S0967-0645(02)00379-X.

Bryden, H. L., L. M. Beal, and L. M. Duncan (2005), Structure and transport of the Agulhas Current and its temporal variability, *J. Oceanogr.*, *61*(1980), 479–492.

Byrne, D. A., and J. L. McClean (2008), Sea level anomaly signals in the Agulhas Current region, *Geophys. Res. Lett.*, *35*(13), L13601, doi:10.1029/2008GL034087.

Chambers, D. P., J. Wahr, and R. S. Nerem (2004), Preliminary observations of global ocean mass variations with GRACE, *Geophys. Res. Lett.*, *31*(13), L13310, doi:10.1029/2004GL020461.

Dahle, C., F. Flechtner, C. Gruber, D. König, R. König, G. Michalak, and K. H. Neumayer (2013), GFZ RL05—An improved time-series of monthly GRACE gravity field solutions, in *Observation of the System Earth from Space - CHAMP, GRACE, GOCE and Future Missions, Geotechnologien Science Report No. 20 Ser.*, edited by F. Flechtner, N. Sneeuw, W.-D. Schuh, Springer, Heidelberg, in press.

Dee, D. P., et al. (2011), The ERA-Interim reanalysis: Configuration and performance of the data assimilation system, *Q. J. R. Meteorol. Soc.*, *137*(656), 553–597, doi:10.1002/qj.828.

Dobslaw, H., and M. Thomas (2007), Simulation and observation of global ocean mass anomalies, *J. Geophys. Res.*, *112*(C5), C05040, doi:10.1029/2006JC004035.

Doglioli, A. M., B. Blanke, S. Speich, and G. Lapeyre (2007), Tracking coherent structures in a regional ocean model with wavelet analysis: Application to Cape Basin eddies, *J. Geophys. Res.*, *112*(C5), C05043, doi:10.1029/2006JC003952.

Doodson, A. T., and H. D. Warburg (1941), *Admiralty Manual of Tides*, 270 pp., H.M. Stationery Office, London.

Drews, C., and W. Han (2010), Dynamics of wind setdown at Suez and the Eastern Nile Delta., *PloS one*, *5*(8), e12481, doi:10.1371/journal.pone.0012481.

Farrell, W. E. (1972), Deformation of the Earth by surface loads, *Rev. Geophys. Space Phys.*, *10*(3), 761–797.

Froyland, G., C. Horenkamp, V. Rossi, N. Santitissadeekorn, and A. S. Gupta (2012), Three-dimensional characterization and tracking of an Agulhas Ring, *Ocean Modell.*, *52-53*, 69–75, doi:10.1016/j.ocemod.2012.05.001.

Han, S.-C., and P. Ditmar (2007), Localized spectral analysis of global satellite gravity fields for recovering time-variable mass redistributions, *J. Geod.*, *82*(7), 423–430, doi:10.1007/s00190-007-0194-5.

Kroner, C., M. Thomas, H. Dobslaw, M. Abe, and A. Weise (2009), Seasonal effects of non-tidal oceanic mass shifts in observations with superconducting gravimeters, *J. Geod.*, *48*, 354–359, doi:10.1016/j.jog. 2009.09.009.

Krug, M., and J. Tournadre (2012), Satellite observations of an annual cycle in the Agulhas Current, *Geophys. Res. Lett.*, *39*(15), L15607, doi:10.1029/2012GL052335.

Kurtenbach, E., T. Mayer-Gürr, and A. Eicker (2009), Deriving daily snapshots of the Earth's gravity field from GRACE L1B data using Kalman filtering, *Geophys. Res. Lett.*, *36*, L17102, doi:10.1029/2009GL039564.

Lutjeharms, J., and D. Webb (1995), Modelling the Agulhas current system with FRAM (fine resolution antarctic model), *Deep Sea Res. Part I*, *42*(4), 523–551, doi:10.1016/0967-0637(94)00031-M.

Lutjeharms, J. R. E. (1981), Spatial scales and intensities of circulation in the ocean areas adjacent to South Africa, *Deep Sea Res. Part A*, *28*(11), 1289–1302, doi:10.1016/0198-0149(81)90035-2.

Lutjeharms, J. R. E., R. Catzel, and H. Valentine (1989), Eddies and other boundary phenomena of the Agulhas Current, *Cont. Shelf Res.*, *9*(7), 597–616, doi:10.1016/0278–4343(89)90032-0.

Macrander, A., C. Böning, O. Boebel, and J. Schröter (2010), Validation of GRACE gravity fields by in-situ data of ocean bottom pressure, in *System Earth Via Geodetic-Geophysical Space Techniques, Adv. Technol. in Earth Sci.*, edited by F. M. Flechtner et al., pp. 169–185, Springer, Berlin, doi:10.1007/978-3-642-10228-8_14.

Meyssignac, B., and A. Cazenave (2012), Sea level: A review of present-day and recent-past changes and variability, *J. Geod.*, *58*, 96–109, doi:10.1016/j.jog.2012.03.005.

Penven, P., J. R. E. Lutjeharms, and P. Florenchie (2006), Madagascar: A pacemaker for the Agulhas Current system?, *Geophys. Res. Lett.*, *33*, L17609, doi:10.1029/2006GL026854.

Penven, P., P. Marchesiello, L. Debreu, and J. Lefèvre (2008), Software tools for pre- and post-processing of oceanic regional simulations, *Environ. Modell. Software*, *23*(5), 660–662, doi:10.1016/j.envsoft.2007.07.004.

Ray, R. D., and D. A. Byrne (2010), Bottom pressure tides along a line in the southeast Atlantic Ocean and comparisons with satellite altimetry, *Ocean Dyn.*, *60*(5), 1167–1176, doi:10.1007/s10236-010-0316-0.

Rietbroek, R., P. LeGrand, B. Wouters, J.-M. Lemoine, G. Ramillien, and C. W. Hughes (2006), Comparison of in situ bottom pressure data with GRACE gravimetry in the Crozet-Kerguelen region, *Geophys. Res. Lett.*, *33*(21), L21601, doi:10.1029/2006GL027452.

Rouault, M., P. Penven, and B. Pohl (2009), Warming in the Agulhas Current system since the 1980's, *Geophys. Res. Lett.*, *36*, L12602, doi:10.1029/2009GL037987.

Schouten, M. W., W. P. M. de Ruijter, P. J. van Leeuwen, and J. R. E. Lutjeharms (2000), Translation, decay and splitting of Agulhas rings in the southeastern Atlantic Ocean, *J. Geophys. Res.*, *105*(C9), 21,913–21,925, doi:10.1029/1999JC000046.

Schouten, M. W., W. P. de Ruijter, P. J. van Leeuwen, and H. Ridderinkhof (2003), Eddies and variability in the Mozambique Channel, *Deep Sea Res. Part II*, *50*(12-13), 1987–2003, doi:10.1016/S0967-0645(03)00042-0.

Shchepetkin, A. F., and J. C. McWilliams (2005), The regional oceanic modeling system (ROMS): A split-explicit, free-surface, topography-following-coordinate oceanic model, *Ocean Modell.*, *9*(4), 347–404, doi:10.1016/j.ocemod.2004.08.002.

Smagorinsky, J. (1963), General circulation experiments with the primitive equations, *Mon. Weather Rev.*, *91*(3), 99–164, doi:10.1175/1520-0493(1963)091¡0099:GCEWTP¿2.3.CO;2.

Song, Y. T., and F. Colberg (2011), Deep ocean warming assessed from altimeters, gravity recovery and climate experiment, in situ measurements, and a non-Boussinesq ocean general circulation model, *J. Geophys. Res.*, *116*(C2), C02020, doi:10.1029/2010JC006601.

Thomas, M., J. Sündermann, and E. Maier-Reimer (2001), Consideration of ocean tides in an OGCM and impacts on subseasonal to decadal polar motion excitation, *Geophys. Res. Lett.*, *28*(12), 2457–2460.

Thompson, K. R., and E. Demirov (2006), Skewness of sea level variability of the world's oceans, *J. Geophys. Res.*, *111*(C5), C05005, doi:10.1029/2004JC002839.

Umlauf, L., and H. Burchard (2003), A generic length-scale equation for geophysical turbulence models, *J. Mar. Res.*, *61*, 235–265, doi:10.1357/002224003322005087.

van Aken, H., A. van Veldhoven, C. Veth, W. P. M. De Ruijter, P. J. van Leeuwen, S. Drijfhout, C. Whittle, and M. Rouault (2003), Observations of a young Agulhas ring, Astrid, during MARE in March 2000, *Deep Sea Res. Part II*, *50*, 167–195, doi:10.1016/S0967-0645(02)00383-1.

van Sebille, E., A. Biastoch, P. J. van Leeuwen, and W. P. M. De Ruijter (2009), A weaker Agulhas Current leads to more Agulhas leakage, *Geophys. Res. Lett.*, *36*(3), 10–13, doi:10.1029/2008GL036614.

van Sebille, E., W. E. Johns, and L. M. Beal (2012), Does the vorticity flux from Agulhas rings control the zonal pathway of NADW across the South Atlantic?, *J. Geophys. Res.*, *117*(C5), C05037, doi:10.1029/2011JC007684.

Wahr, J., M. Molenaar, and F. O. Bryan (1998), Time variability of the Earth's gravity field: Hydrological and oceanic effects and their possible detection using GRACE, *J. Geophys. Res.*, *103*(B12), 30,205–30,229, doi:10.1029/98JB02844.

Wieczorek, M. A., and F. J. Simons (2005), Localized spectral analysis on the sphere, *Geophys. J. Int.*, *162*(3), 655–675, doi:10.1111/j.1365-246X.2005.02687.x.